ZURICH UNIVERSITY OF APPLIED SCIENCES
SCHOOL OF LIFE SCIENCES AND FACILITY MANAGEMENT
INSTITUTE OF NATURAL RESOURCES SCIENCES (IUNR)

Integration of Surface Albedo Change in the Life Cycle Assessment of Photovoltaic Systems

Earth Observation Data for Environmental Impact Modelling

PWRG 2

by
Michlmayr, Elke
MSc Environment and Natural Resources
Submitted: Jan 21, 2026

Supervisor:
Itten, René
ZHAW School of Life Sciences and Facility Management

Abstract

Remote sensing, in particular satellite-based earth observation (EO), provides extensive datasets that hold potential for supporting life cycle assessments (LCA) to evaluate environmental impacts across a product or service life cycle. This project work suggests an approach for integrating remote sensing data to enhance the accuracy of environmental impact evaluations in various stages, especially in the inventory and modelling phases.

A promising area where such data might be applied is for the evaluation of changes in surface reflectivity (albedo) associated with the installation of photovoltaic panels (PV). This can be assessed from the relevant satellite data of the PV sites under study and some reference data to compare it to, for both building mounted PV panels and open ground PV installations in deserts, on grasslands, on croplands, or on water surfaces. The change in surface albedo caused by replacing natural or built surfaces with PV panels is presumed to constitute a measurable effect that can potentially be quantified and incorporated into an LCA. Depending on the type of land cover, there might be net positive, neutral, or net negative effects.

The outcome of a literature study performed is that, while surface albedo change is a measurable environmental effect of PV installations, it plays a minor role compared to the overall benefits of renewable energy. The magnitude of impact on surface albedo is dependent on the original land cover being replaced, with installations on dark-roofed buildings showing negligible changes, whereas alpine and desert environments experience the most pronounced reductions in reflectivity. Despite the local warming induced by these changes, the positive radiative forcing caused by albedo reduction is typically offset by the clean energy generation provided by the PV plant.

The paper contributes a two-tiered methodology to integrate the environmental impact of surface albedo changes of PV installations into an LCA.

1 Introduction

Albedo is the ratio of solar energy reflected by a surface. Light surfaces (e.g. snow and ice) reflect a large portion of the sunlight while dark surfaces like asphalt do not reflect it but instead absorb the sunlight and convert it into heat. Therefore, when the albedo of the earth's surface or atmosphere changes, the planet's energy balance is altered. The planetary boundaries framework by Richardson et al. (2023) lists surface albedo changes after greenhouse gases and aerosols as the third key anthropogenic driver in the climate change category, which is measured in (1) atmospheric CO_2 concentration and (2) energy imbalance at the top of the atmosphere. The change in the balance between incoming and outgoing energy is known as radiative forcing (RF). This effect drives weather patterns, surface temperatures, and consequently, the climate system.

Solar panels convert sunlight into both electrical energy and heat. Since PV installations typically replace existing surfaces with lower-albedo PV modules, they alter the surface reflectivity and, consequently, the local and global energy balance.

Life Cycle Assessment (LCA) is a standardized tool used to evaluate the environmental impacts associated with every stage of a product or service's life, from raw material extraction through production, use, and disposal (International Organization for Standardization, 2006a) (International Organization for Standardization, 2006b). Central to the accuracy and usefulness of an LCA is the availability and quality of the underlying data. Typically the data originates from databases with collected background data such as ecoinvent (ecoinvent Centre, 2023). However, the data required to assess albedo-related effects, such as surface reflectance and related radiative forcing contributions, is not included in ecoinvent or other comparable LCI databases, and albedo-related effects for PV installation are currently not included.

Remote sensing, particularly through satellites, provides vast amounts of spatial data. Satellites offer a unique, large-scale perspective for continuous observation of the earth's surface and atmosphere. They collect data that can be directly or indirectly used to assess land cover, vegetation health, surface temperatures, atmospheric gases, and ocean characteristics. All of these are essential for understanding environmental trends and changes over time. Satellite-derived earth observation (EO) data is continuously collected and supports a wide range of applications, from climate modelling and disaster response to agricultural planning. In particular, EO data allows (1) to assess if a certain location is currently covered by a solar panel, and (2) measure the reflectivity in that location before and after the installation. While ISO14040 (International Organization for Standardization, 2006a) provides the necessary structure for an LCA, it refrains from dictating specific methodological approaches for emerging or complex environmental phenomena, such as the albedo effect and radiative forcing. This absence of prescriptive methods allows for the integration of additional data sources, e.g EO data, in an LCA.

The aim of this work is to describe how to (1) quantify the environmental impact of albedo changes associated with dark coloured PV installations and (2) integrate it into an LCA for photovoltaic systems. Three sets of research questions will be explored:

1. How can satellite-derived remote sensing data be applied to assess changes in surface albedo resulting from PV installations by comparing its effects before and after the installation? What level of spatial and temporal data aggregation is required to obtain meaningful results, given the quality and resolution of the data? The hypothesis is that the inherent noise found in satellite-derived remote sensing data (e.g. due to varying weather conditions and cloud cover) along with its limited spatial resolution will represent major constraints to be dealt with. Nevertheless, it is expected that it will be possible to derive statistically significant result estimates with appropriate data processing and statistical methods.
2. How does the original surface of PV systems, such as building or open ground, influence the amount of albedo change from the installation? Is it feasible to identify the original

surface such as buildings, deserts, grasslands, croplands, water? Is it possible to assess and quantify the albedo change by original surface type? Furthermore, is seasonality (e.g., temporal snow cover and vegetation dynamics) a relevant factor? The hypothesis is that the impact will depend on the original surface being replaced. Albedo changes for building mounted PV panels are likely to be minor, since the albedo of typical dark roofing is expected to be similar to that of a solar panel surface. However, for other surfaces such as deserts, the changes in albedo might be significant.

3. How can the satellite-derived data be incorporated into an LCA in a methodologically sound and credible manner, enabling its authoritative use in environmental impact assessments of solar energy systems? The hypothesis is that satellite-derived datasets from sources such as U.S. National Oceanic and Atmospheric Administration (NOAA) or European Organisation for the Exploitation of Meteorological Satellites (EUMETSAT) are considered reliable and scientifically validated. The expectation is that the given data quality should allow for quantifying aggregated albedo changes by original surface type and consequently support the incorporation of these effects into an LCA for a photovoltaic system.

The structure of this project work is as follows. First, there is an introduction with a formulation of the research questions. After that, a review of existing literature is presented, focusing on how albedo changes are incorporated into an LCA and how remote sensing–based metrics can support this integration. Subsequently, the required data inputs and the methodological steps to address the research questions are described followed by a section to conclude and discuss the work.

2 Literature review

Several research areas relate to the research questions explored, including albedo effects in general, albedo effects of photovoltaic (PV) systems, the inclusion of albedo effects in an LCA, and remote sensing applications for a location-specific LCA. This chapter provides an overview of existing studies in these fields that are relevant to the present work. Most of the studies that deal with surface albedo use spatially explicit data.

2.1 Albedo effects compared between surfaces and on the hemisphere level

Hasler et al. (2024) find that maximizing the climate benefits of tree cover restoration requires accounting for albedo effects since they often offset or even reverse carbon removal gains, especially in dryland and boreal regions. Using spatial data, the study shows that while many restoration projects target climate-positive areas, many face an albedo offset of at least 20%. The study suggests rolling out large-scale tools to identify areas where restoration delivers net climate benefits.

Zhu et al. (2024) indicate the significant impacts of climate change and human disturbances on East Asia grassland ecosystems from the perspective of altered albedo. Changes in vegetation greenness and soil properties have a substantial impact on albedo.

Wu et al. (2024) estimate a 30 meter resolution annual surface albedo dataset for more than 3000 large cities worldwide for the period from 1986 to 2020 from the Landsat surface reflectance product (see Survey (2020)) and find an overall decreasing trend of albedo during the 35-year evaluation period, which is robust accounting for uncertainties from training sample representativeness, data uncertainty, seasonal variation, and snow-cover contamination.

Loeb et al. (2025) use 24 years of satellite observations to show that there is a small measurable difference between the Northern and Southern Hemispheres in both absorbed solar radiation (ASR) and outgoing longwave radiation (OLR). The emerging darkening of the Northern Hemisphere relative to the Southern Hemisphere is linked to changes in aerosol radiation interactions, surface albedo, and water vapor distributions. This hemispheric asymmetry in radiation is closely connected to variations in the atmosphere and ocean general circulation. The assumption so far was that changes in cloud cover would balance the differences between the hemispheres (see Datseris and Stevens (2021)), but this study suggests that this compensating effect is not completely effective. Understanding how the clouds respond to the developing imbalance is critical for predicting future climate evolution. Diamond et al. (2024) follow up on this line of research by breaking down the hemispheric albedo symmetry into components associated with the surface, clear-sky atmosphere, and different cloud types as defined by cloud effective pressure and optical thickness.

2.2 PV installations and albedo effects

Today's solar panels are all in the typical dark colour. Efforts to improve the performance of coloured panels, such as those described by Ji et al. (2019), are ongoing and will take time to reach practical application. At this point in time, if architects want to use lighter colours, which happens especially for facade installations, this has to be realised by installing lighter coloured glass panels in front of the dark solar panel. Doing so reduces the amount of albedo change but also the overall energy yield from the PV installation.

Barron-Gafford et al. (2016) found that PV farms induce a "heat island" effect when lowering the terrestrial albedo from ~20% in natural deserts to ~5% over PV panels by installing a PV farm. Temperatures were regularly 3–4 °C warmer than the surrounding wildlands at night. On the contrary, Zhang and Xu (2020) analyzed surface temperature changes at the 23 largest PV installations worldwide using thermal infrared remote sensing. They found that the PV plants significantly reduced daily mean surface temperature by ~0.5 °C, with a stronger cooling effect during the daytime than at night, and that cooling intensity increased with plant capacity. Although PV installation lowered surface albedo, it increased effective albedo when electricity generation was considered because PV systems convert a portion of the absorbed solar radiation into electricity, which is exported away from the site rather than

being released locally as heat. The magnitude of cooling, especially at night, varied with latitude, elevation, climate, and vegetation conditions, suggesting that regional geography and environment should be considered when selecting future PV plant sites.

Coimbra (2025) focused on thermal effects of solar plants on the environment and vice-versa. Large-scale solar power plants are often built in arid or desert habitats with fauna and flora that are highly sensitive to changes in temperature and humidity. Not only albedo change, but also many other factors such as wind direction and speed, dust concentration, ground condition, panel configuration density, orientation and distribution throughout the solar field, affect the local environment, the balance between radiation and convection, and in turn, the performance and thermal impact of solar power plants.

2.3 Albedo effects of PV installations per original surface

Other studies investigated the impact of PV on radiative forcing at several different installation sites such as city roofs, deserts, alpine locations, and lakes:

- Zhou et al. (2025) used a LiDAR-based approach to quantify urban albedo for the city of Delft assuming that all appropriate roofs would be covered with PV panels and found that this would yield 485.72 GWh of electric energy per year, while it would minimally lower the city's albedo and impose $3.53 * 10^{-8} W\, m^{-2}$ positive RF. The results were validated using MODIS satellite observations.
- Z. Li et al. (2022) examined the effects of PV panels on surface radiation through a comparative study between a PV site and a reference site in the Gobi area of Xinjiang, China in summer 2020. The results showed that nighttime outgoing longwave radiation (OLR) was lower at the PV site, while daytime values were similar. The PV site's surface albedo (0.14) was 39.1% lower than the reference site's (0.23). Overall, net radiation was 30.7% higher at the PV site: 75% due to reduced upward shortwave radiation, and 25% to lower nocturnal longwave radiation.
- Wang et al. (2025) studied PV installations in an alpine meadow on the eastern Tibetan Plateau and found a 28.9% increase in net radiation, but reduced albedo and wind speed by 31.6% and 36.2%, respectively. Air temperature rose in daytime and summer, but dropped at night and in winter. Soil under panels was colder and drier, while gaps were colder and wetter, extending the frozen period by roughly 50 days and slowing moisture loss up to 3.5×. These shifts alter local energy and water balances and may moderate climate warming impacts, warranting further studies to evaluate the long-term impacts on vegetation dynamics and permafrost processes.
- P. Li et al. (2022) examined fishery complementary PV plants using a physical model to reveal their microclimatic effects. Deployment turned the lake into a heat sink, reducing albedo by 18.8%. Water energy change was driven by a water/air vapor pressure

deficit. Also, the panels warmed the surrounding environment, with heating intensity depending on water depth and strongest at the surface.

- S. Zhao et al. (2025) compared white roofs and PV roofs and showed that economic payback periods for (white) cooling roofs and PV roofs are 1.75 years and 10.90 years, respectively; the energy payback periods are 13.6 years and 43.7 years, respectively; and the environmental payback periods are 2.2 years and 7.6 years, respectively. In terms of energy savings, photovoltaic roofs outperform cooling roofs significantly, with an annual energy saving of 139 kWh/m² for photovoltaic roofs compared to 6.5 kWh/m² for cooling roofs.

In conclusion, impacts on albedo caused by PV installations were observed on all these surfaces, and these impacts could potentially be included in an LCA.

2.4 Albedo effects of the surroundings of PV installations

Gul et al. (2018) examined the effects of the surfaces around PV installation and found that these have a small effects on the performance. It is preferrable to use bright, reflective materials like white tiles around PV panels since these maintain higher and more stable albedo values, especially in cloudy northern regions where ground reflection contributes significantly to total solar gain.

Cosgun and Demir (2024) explored the performance of floating PV modules installed over water surfaces, focusing on their efficiency and environmental benefits. A 1 MW PV system was simulated with two types of PV modules, bifacial and monofacial, both mounted 1 meter above the water. Results showed that bifacial modules generated more energy annually than monofacial ones due to enhanced albedo reflection from the water surface.

Lavaert et al. (2023) investigated how different ground covers affect the electricity production of two agrivoltaic systems: fixed vertical bifacial panels and horizontal single-axis trackers. The study aimed to determine whether reflective ground covers, such as white cloths, could enhance light capture and energy generation. Simulations suggested that the white ground cloth could increase the incident irradiance on the vertical bifacial panels by about 8%, but real-world measurements over 5.5 months showed no significant difference between ground covers. In contrast, for the horizontal single-axis tracker system, there was a clear benefit with the white ground cloth leading to higher yields.

2.5 Albedo effects in LCA studies

Several studies from the LCA research community have attempted to quantify albedo-related effects for inclusion in an LCA:

- Susca (2012) proposed an enhancement of the LCA methodology with a time-dependent climatological model for including the effect of surface albedo on climate. They evaluated their theoretical findings with a case study of a black and a white roof evaluated over the timeframes of 50 and 100 years. The comparative LCA of the two roofs showed that the high surface albedo of the white roof played a crucial role in offsetting RF.
- David et al. (2025) assessed whether accounting for surface albedo change caused by land use change in carbon credit quantification methods influences the amount of credits and found that overcrediting can happen because planting trees can darken the land.
- Jungbluth et al. (2012) presents collected data on the albedo effects from various surfaces including PV panels. While the direct impact on global radiative forcing is considered minimal, local albedo changes induced by large PV installations could have minor implications for nearby ecosystems and microclimates.
- Bright et al. (2012) examine two key dynamic factors affecting bioenergy's climate impact: temporary changes in the terrestrial carbon cycle, and land surface albedo. The paper proposes ways to integrate these factors into LCA. Using a case study of transportation biofuel from managed boreal forests in northern Europe, the authors develop global warming potential (GWP) indices for different land management scenarios, highlighting the need for region-specific characterization factors and discussing related uncertainties.
- Cai et al. (2016) quantified land use change (LUC) induced albedo effects from large-scale U.S. biofuel production and compared them with greenhouse gas emissions from traditional lifecycle analyses. Using over 1.4 million satellite albedo observations across six Agro-Ecological Zones, paired with high-resolution crop data, they modeled radiative forcing related impacts of LUC for seven crop types. Results show average albedo effects of −1.8 g CO_2-eq/MJ for corn ethanol (cooling), +2.7 g CO_2-eq/MJ for miscanthus, and +12.1 g CO_2-eq/MJ for switchgrass (warming). Strong spatial variability indicates that biofuel climate impacts depend heavily on local land and vegetation characteristics.

One of the earliest studies examining the environmental impacts of photovoltaic (PV) installations is Fthenakis et al. (2008), and since then, numerous scientific publications have investigated PV systems through LCA approaches. While most of them overlook the effects of surface albedo change, a limited number of studies have attempted to quantify the effect in a way that could be used as in input to an LCA:

- Nemet (2009) estimated the effects of covering the earth with sunlight-absorbing panels on a large scale and therefore reducing surface albedo. They found that avoided emissions from PV generated energy were far greater than the observed warming effect from the related albedo reduction.
- Wei et al. (2024) confirmed these results based on global satellite data, and also showed that albedo-induced positive radiative forcing can be offset by negative radiative forcing from clean solar generation in most PV farms within one year.

- Xu et al. (2024) performed a global assessment of the effects of solar farms on albedo and vegetation for 116 large solar farms using MODIS data. They demonstrated that the installation of these farms decreased the annual mean surface shortwave albedo and reduced the enhanced vegetation index (EVI) relative to the surrounding areas. The greatest impacts on albedo were observed in barren land, followed by grassland and cropland, while the opposite order applied for vegetation impact. In terms of seasonal and latitudinal variations, the largest impact on albedo was observed at high latitudes in winter.

2.6 Spatially explicit LCA studies

A spatially explicit LCA is a refinement of a traditional LCA to incorporate geographical and location-specific information into the assessment of environmental impacts. The key difference is the use of location-specific inventory data for different purposes, such as road infrastructure planning as described by Karlsson et al. (2017). Geographic Information Systems (GIS) and remote sensing are often used to map and quantify regional effects.

J. Li et al. (2021) provide a meta study of 105 publications on GIS-based LCA studies and propose a universal methodological framework to address the following issues: (1) setting up a geographically referenced system in the goal and scope definition phase; (2) spatializing lifecycle data and integrating and computing foreground and background data in the inventory analysis phase; (3) developing spatialized characterization factors with different requirements on resolution and data availability in the impact assessment phase; and (4) harmonizing the contribution analysis of different zones, unit processes, and elementary flows to visualize the spatialized environmental footprint in the interpretation phase.

Itten et al. (2023) explore how remote sensing data from satellites can support and partly replace company-provided data for scope 3 greenhouse gas reporting to improve transparency and enable comparisons. The interdisciplinary research group identified remote sensing data sources for agriculture, mining, and energy sectors. Commercial providers already offer relevant ESG-oriented remote sensing based data products based on processed satellite imagery. These datasets on land use change (most recently by Jian et al. (2025)), biodiversity, and biomass carbon can enable regionalized and consistent LCI models across larger areas and time periods.

Reinhard et al. (2016) provide a case study for integrating regionalized life cycle inventory modelling in an LCA for rapeseed cultivation in Germany based on rasterized inventory data with a resolution of one kilometer following the methodological guidelines for the life cycle inventory of agricultural products developed by Nemecek et al. (2014).

Dorber et al. (2018) uses satellite data to estimate the environmental impact from land use and land use change for hydropower reservoirs for application in an LCA. The study calculated an average net land occupation for water storage reservoirs in Norway, with an adjustment to account for the natural lakes that were often part of the reservoirs' area before impoundment,

for a more comprehensive evaluation of the overall environmental footprint of hydroelectric power.

Geyer, Stoms, et al. (2010) present an inventory modelling proof-of-concept approach for coupling GIS and LCA for biodiversity assessments of land use and applies it to a case study of ethanol production from agricultural crops in California, and a follow up for impact assessment in Geyer, Lindner, et al. (2010).

2.7 Relevant satellite-derived datasets and tools for surface albedo

Roccetti et al. (2024) provide a dataset for surface albedo based on the MODIS Surface Reflectance Black-Sky Albedo dataset (see Schaaf and Wang (2021)) and principal component analysis (PCA) as described by Hotelling (1933).

Riihelä et al. (2024) present CLARA-A3 surface albedo data as the third edition of the CM SAF Cloud, Albedo and surface Radiation (CLARA) data record family. The temporal coverage of this edition is extended from 1979 until the near-present day. The core algorithms and data format remain unchanged from previous editions, but now white- and blue-sky albedo estimates are also available for the first time in CLARA data.

Cloud cover constitutes a major challenge for surface albedo estimation. Manninen et al. (2022) describe a new method for cloud-correcting observations of black-sky surface albedo derived using Advanced Very High Resolution Radiometer (AVHRR) data for all possible conditions of cloud fraction and cloud type with any land cover type and solar zenith angle.

2.8 Accuracy of satellite-derived data

The accuracy of satellite-derived data is crucial for any use case depending on it. Many scientific publications are focused on assessing accuracy levels of satellite-derived data and understanding the reasons for any discrepancies:

- Gruber et al. (2020) propose good practice guidelines for the validation of global coarse-scale satellite soil moisture datasets and practical recommendations on data preprocessing and presentation of statistical results together with a recommended validation protocol and an example validation.
- Langsdale et al. (2025) review key challenges in validating satellite ECVs across terrestrial, oceanic, and atmospheric domains. They focus on issues with reference data, their use in validation, and comparison methods and provide recommendations for improving uncertainty modelling, transparency about data limitations, metadata management, and best practices for validation methodologies.

- Paris et al. (2023) discuss issues caused by inconsistencies between the actual data and the information derived from satellite data that can be attributed to factors such as differences in viewpoint perspectives, i.e., aerial versus ground views, or spatial resolution of the satellite images versus the extent of the land cover present in the scene.
- Tran et al. (2023) reviewed 676 papers written between 2011 and 2021 on uncertainty assessment of remote sensing-based evapotranspiration data (RS-ET), categorizing the approaches taken by methods, context, and reporting metrics. They found that assessments are inconsistent in methodology, reference data, geographic coverage, and uncertainty reporting. The study recommends that future work should clearly document validation context, reference data uncertainties, spatial and temporal mismatches, and report multiple performance metrics.

3 Materials and methods

Section 3.1 describes how relevant satellite data can be retrieved and processed to determine the change in surface albedo (delta) caused by PV installations. Section 3.2 outlines the principles and methods used to measure surface albedo and describes its relationship with radiative forcing, which is needed to quantify the environmental impact of albedo changes. Section 3.3 discusses the considerations arising from the original surface that was replaced by the PV panels, and the implications on surface albedo. Section 3.4 discusses how to translate the resulting data into an environmental impact assessment, and how to include these results in an LCA.

3.1 Retrieving and processing remote sensing data

Satellite remote sensing provides a spatially continuous means of estimating surface albedo. The spatial areas of interest where the PV plant(s) are located will be defined based on the investigated use case. All the data points that (completely and/or partly) cover the relevant area will be selected. This process can be supported with image recognition techniques (e.g. a deep learning model for detecting solar panels), or it can be based on defined location data.

Satellite-derived data inherently contains significant noise due to variable weather conditions, cloud cover, and operational factors. To quantify the change in albedo (delta), two comparison approaches can be used: (1) comparing the PV farm area with itself prior to installation, or (2) comparing it with a nearby reference area of the same size and surface characteristics as the original land replaced by the PV installation. The second approach is preferable, as the data points from both areas are subject to the same weather conditions and operational influences, whereas in the before-and-after scenario, the temporal conditions differ which would influence the results to a large extent.

Many satellites provide relevant data (see Section 5.3 for a full overview). In this section, the most appropriate are identified. One of the main considerations is the data resolution (minimum square pixel size available) required, which depends on the use case. It's also important to choose data that is in the public domain. Also relevant is the time frame for which the required data is available.

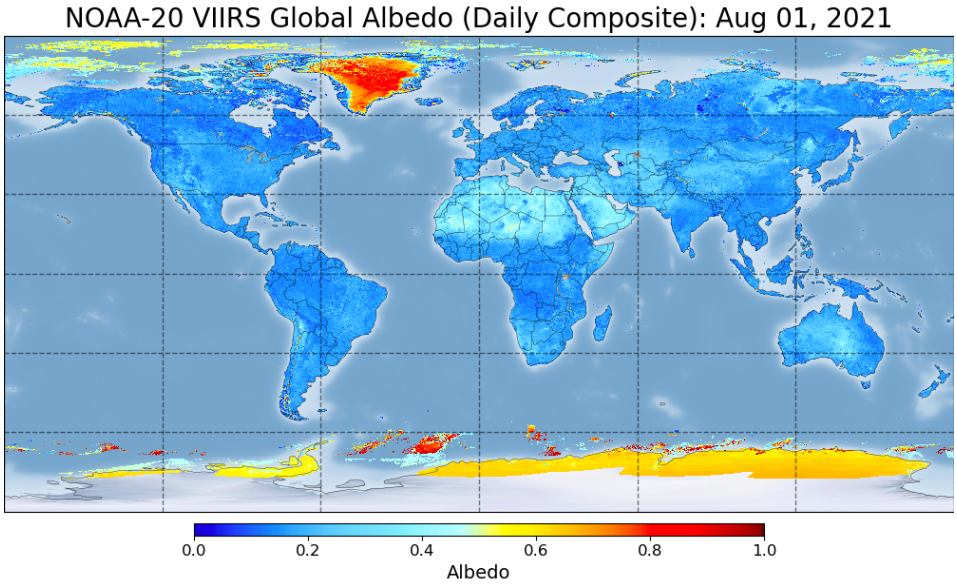

Figure 1: Global map with surface albedo data from VIIRS satellite. Source: National Oceanic and Atmospheric Administration (NOAA)

Some satellites, such as MODIS and VIIRS, provide instruments for direct albedo monitoring (e.g., MODIS MCD43A3, VIIRS VNP43). An example for data generated by VIIRS in August 2021 is shown in Figure 1. Since the resolution from these satellites is generally coarse with 500 to 750 meters, the resulting data can only be applied for very large PV farms.

Other satellite types provide higher spatial resolution and therefore can also be used to assess smaller PV sites. They employ multi-spectral sensors to record surface reflectance across different wavelengths (e.g., shortwave, visible, or near-infrared). The albedo can then be derived by applying weighted linear combinations of these reflectance values. Examples for this category are Landsat and Sentinel-2. Their spatial resolution is between 10 and 60 meters. Sentinel-2 data is available from 2015 onwards, and Landsat data from 1984 onwards (for use cases where longer history is required).

The selected data can then be downloaded for further processing and analysis. These datasets are typically very large and are continuously updated over time (e.g. every 10 minutes). Therefore, appropriate data management and downloading tools should be used to ensure efficiency and reliability.

3.2 Albedo measurement and radiative forcing

Albedo is defined as the ratio of reflected to incoming solar radiation: $\alpha = \frac{R_{reflected}}{R_{incoming}}$

It is a unitless quantity that can range between 0 for complete absorption to 1 for complete reflection. The albedo value of any location depends on the surface material, texture, colour, and the angle of incoming solar radiation. Ground-based albedo can also be measured using pyranometers or albedometers (e.g., mounted on towers) recording incoming and reflected shortwave radiation over a defined area. Although they are highly accurate, the ground-based measurements are limited in spatial coverage and therefore the satellite-based approach is deemed preferable for LCA integration.

Radiative forcing (RF) is generally measured in watts per square meter ($W\ m^{-2}$) and quantifies the change in the earth's energy balance resulting from modifications to the incoming or outgoing radiation. There are many factors that can cause such a modification: Emission of greenhouse gases such as CO_2 or CH_4, aerosols such as black carbon, land use changes and therefore albedo changes (focus of this work), and solar variability which are the natural fluctuations in the amount of solar radiation reaching the earth over time. The IPCC AR6 report by Forster et al. (2021) assessed the contributions as presented in Table 1 below:

Table 1: Radiative Forcing contributions per category from IPCC AR6 report

Category	Radiative Forcing (2019 vs. 1750)
Carbon dioxide CO_2	+2.16 W/m²
Methane CH_4	+0.54 W/m²
Nitrous oxide N_2O	+0.21 W/m²
Halogenated gases	+0.32 W/m²
Ozone O_3	+0.47 W/m²
Aerosols	−1.10 W/m²
Land use change related albedo change	−0.15 W/m²
Contrails and aviation induced cirrus	+0.05 W/m²
Solar variability	+0.01 W/m²
In total	≈ +2.72 W/m²

Positive RF is the initial driver of climate change. It causes temperature rise in the atmosphere and on the earth surface (sea and land). Temperature rise causes ice-covered regions such as ice sheets, glaciers, and sea ice to melt. This is a positive feedback loop for further albedo changes, since bright surfaces are replaced by darker ones. Changes in surface albedo directly modify the shortwave component of the radiative balance. A reduction in albedo (e.g., replacing bright desert surface with dark PV panels) increases the absorption of solar energy, leading to positive radiative forcing (surface warming). Conversely, an increase in albedo contributes

to negative radiative forcing (surface cooling). Table 1 contextualizes the radiative forcing resulting from overall land-use-change-related albedo changes, showing that, when considering all land-use changes (not just PV-related), the net effect of these albedo changes is cooling.

The radiative forcing impact ΔF caused by an albedo change $\Delta\alpha$ can be approximated as:

$$\Delta F = -S \cdot (1 - A) \cdot \Delta\alpha/4$$

where the solar constant S is equal to ~1361 $W\ m^{-2}$ and the planetary albedo A amounts to ~0.3 (this is an empirically derived value from satellite measurements for the entire earth). The factor of ¼ accounts for the ratio of the earth's cross-sectional area to its total surface area, since only the planet's disk intercepts sunlight. This means that the intercepted energy must be averaged over the entire surface area of the earth to express the impact per unit area globally. Negative values of ΔF represent cooling (because of increased reflectivity), while positive values indicate warming (because of decreased reflectivity).

3.3 Original surface detection and related albedo values

For identifying the original surface there are several relevant satellite-based datasets such as Zanaga et al. (2022), which is based on aggregated Sentinel data from 2021. It provides the surface type for each 10x10 meter square globally. The surface categories provided are described in Table 2. Table 3 provides a list of aggregated albedo values per surface type derived from on satellite data (MODIS, Meteosat) together with a reference to the origin for each value.

Table 2: ESA WorldCover (10 m resolution global land cover map) categories from Zanaga et al. (2022)

Class	Description
Tree cover	Areas dominated by trees (≥10% cover), incl. plantations and flooded forests.
Shrubland	Areas dominated by shrubs (<5 m tall) with ≥10% shrub cover.
Grassland	Areas dominated by herbaceous plants (≥10% cover); woody plants <10%.
Cropland	Land where plants are sown or harvested at least once a year.
Built-up	Land covered by buildings, roads, and other man-made structures.
Bare and sparse vegetation	Lands with exposed soil, sand, or rocks, and ≤10% vegetative cover.
Snow and ice	Areas persistently covered by snow or glaciers.
Permanent water bodies	Lakes, reservoirs, and rivers mostly covered by water (>9 months/year).

Class	Description
Herbaceous wetland	Land dominated by herbaceous vegetation, permanently or regularly flooded.
Mangroves	Salt-tolerant trees and plants in intertidal tropical zones.
Moss and lichen	Land covered by mosses and/or lichens, often in polar or high-altitude regions.

Table 3: Compiled list of typical albedo values per surface type

Surface type	Mean yearly albedo	Source
Deep water	0.04–0.08	Brutsaert (1984)
Moist dark soils / ploughed fields	0.05–0.15	Brutsaert (1984)
Water	~ 0.1	Oke (1987)
Buildings (dark roof)	~ 0.1	Oke (1987)
PV panels	~ 0.1	Argonne National Laboratory (2012)
Asphalt	~ 0.1	Moretti et al. (2021)
Evergreen needleleaf forest	~ 0.11	Cescatti et al. (2012)
Evergreen broadleaf forest	~ 0.13	Cescatti et al. (2012)
Mixed forest	~ 0.13	Cescatti et al. (2012)
Coniferous forest	0.10–0.15	Brutsaert (1984)
Grey soils or bare fields	0.15–0.25	Brutsaert (1984)
Deciduous broadleaf forest	~ 0.14	Cescatti et al. (2012)
Woody savanna	~ 0.18	Cescatti et al. (2012)
Savanna	~ 0.21	Cescatti et al. (2012)
Grass or short vegetation	0.15–0.25	Brutsaert (1984)
Grassland	~ 0.22	Cescatti et al. (2012)
Cropland	~ 0.23	Cescatti et al. (2012)
Dry soils or desert	0.20–0.35	Brutsaert (1984)
White sand	0.30–0.40	Brutsaert (1984)
Desert sand	~ 0.4	Tetzlaff (1983)
Melting snow	~ 0.4	Van Dalum et al. (2020)
Old or dirty snow	0.35–0.65	Brutsaert (1984)
Clean snow	0.60–0.75	Brutsaert (1984)
Older snow or firn	~ 0.7	Van Dalum et al. (2020)
White roof coating	~ 0.75	U.S. Environmental Protection Agency (2003)
Fresh dry snow	0.80–0.90	Brutsaert (1984)

3.4 LCA integration

This section describes how to incorporate satellite-derived surface albedo change data into an LCA in a methodologically sound manner for data methodology and impact metric assessment.

3.4.1 Data methodology

Two potential approaches are described, for PV site specific data and for generalized data. These approaches may be combined within a hierarchical (stacked) framework, whereby the most appropriate method is applied depending on data availability and intended use case.

3.4.1.1 PV site specific data

Figure 2 provides an overview of the steps required for LCA integration for PV site specific data, which will be described in this section.

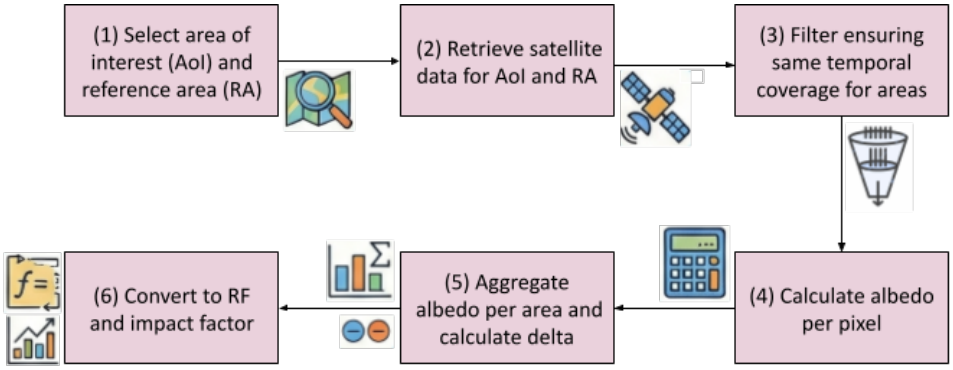

Figure 2: Methodology for PV site specific data integration in LCA

As the first step (1), the relevant data for the area of interest (AoI) and the reference area (RA) will be selected (see Section 3.1). After that in (2) the data will be retrieved, usually via download from the satellite provider. In the next step (3), faulty data points in the downloaded data need to be identified and filtered out. To ensure comparability of the AoI and RA data in the later steps, it is required that both data sets are filtered in the exact same way and that they have the exact same temporal coverage.

These datasets then build the base for calculating albedo values in step (4) as described in Section 3.2. There will be one result value for each minimally supported geographical location (square pixel) from the relevant satellite bands. This calculation is satellite specific, since it is based on the bands provided, and each satellite provides different band setups. Relevant satellite band specific formulas are provided in Liang (2001). The next step is to aggregate all

the per-pixel data for the same pixel to combine them to an average per-pixel result. From these individual numbers, an average result for the whole area (AoI or RA) can be determined. Aggregation steps reduce noise progressively the more data is combined. Consequently, the resulting estimates will be more stable the larger the PV plant, and the longer the observation period. Step 5 and 6 are described in Section 3.4.2.

While this approach uses the most specific data possible, there are two major limitations. Most importantly, note that the suggested approach is only applicable for PV farms that are already installed, because the relevant satellite data will not exist otherwise. In addition, since seasonal factors such as temporal snow cover and vegetation dynamics in the location will play a role for many spatial areas of interest, the temporal aggregation window must be at least one year. This means that only PV plants that already exist for longer than that period can be evaluated instantly.

3.4.1.2 Generalized data

Given the constraints described for PV site specific data, a more practical approach could be to provide generalized data rather than PV site specific values. LCA methodologies typically rely on aggregated impact factors, which can be globalized or regionalized. To enable its authoritative use in environmental impact assessments, any impact factor should best be published by independent bodies such as government agencies, research institutions, or expert panels.

Although this approach cannot capture the high spatial variability inherent to the PV site's environmental conditions (e.g., sun angle, climate, surrounding environment) or the PV system characteristics (e.g., panel tilt, orientation, colour, and coating), estimating the albedo change using general values for the albedo of PV panels and the original surface is expected to result in a reasonable estimate. It can be implemented in a globalized or regionalized way, depending on the extent of influence of environmental conditions and PV system characteristics on the impact factors. Figure 3 depicts how to implement this approach for the given use case.

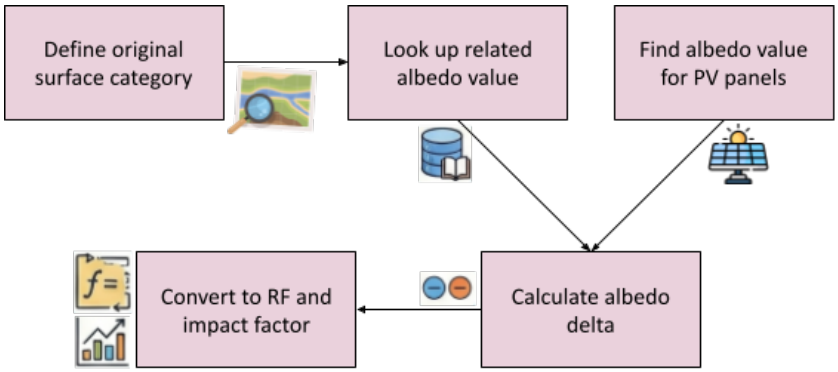

Figure 3: Methodology for generalized data integration in LCA

In this case, the original surface can either be specified by the user or identified using processed satellite data such as the ESA WorldCover from Zanaga et al. (2022). The corresponding estimate for the surface albedo will be gathered from literature study as already compiled in Table 3.

3.4.2 Impact metric assessment

The final outcome of the aggregation steps described in the previous section are two average albedo values, one for the area of interest and one for the reference area. These two numeric numbers between 0 and 1 are the input to the delta calculation of the albedo change. The result is a very small scalar $\Delta\alpha$, which will be converted into a radiative forcing (RF) value ΔF as described in Section 3.2.

The RF value will be translated into a comparable impact metric, enabling direct comparison with other climate impacts and integration into an LCA. The most relevant impact category for radiative forcing is its global warming potential (GWP) over time. To calculate it, the RF is time-integrated to account for the cumulative effect over a chosen time horizon (commonly 20, 50, or 100 years). This will result in an absolute number for the cumulative radiative energy change in the earth's atmosphere system for the chosen time horizon. The absolute number will be normalized by comparing it to CO_2 to receive CO_2-equivalent emissions (CO_2-eq).

For an LCA for a PV farm, the functional unit will typically be a certain amount of electric power such as a kilowatt-hour (kWh), and the most relevant impact metric will be climate change expressed in CO_2-eq per kWh of produced power. This allows for easy integration of the additional impact from the surface albedo change in the LCA by incorporating the associated CO_2-eq contribution per functional unit.

4 Discussion and conclusion

In this paper, a methodology for integrating surface albedo changes in an LCA via satellite or generalized data has been presented. The site-specific approach utilizes a six-step framework that begins with selecting an area of interest and a reference area, followed by retrieving and filtering high-resolution satellite imagery to ensure identical temporal coverage. Albedo is then calculated at the pixel level and aggregated to determine the average delta ($\Delta\alpha$) between the PV installation and the original land cover. Finally, the result is converted to an amount of radiative forcing, from which an impact factor can be derived. Alternatively, the generalized approach offers a simplified application by identifying the original surface through existing global datasets and applying albedo values derived from literature to estimate the change relative to dark coloured PV panels.

The compiled surface albedo values in Table 3 reveal substantial variation among different surface types. Because the albedo of PV panels is comparable to that of buildings with dark

roofs, installing PV systems on such buildings results in only minor changes in surface albedo. Water surfaces have a slightly lower albedo than PV panels, meaning that floating PV installations will lead to a small increase in albedo. In contrast, desert sand exhibits a higher albedo than PV panels, therefore large-scale PV farms in desert environments are expected to induce a moderate reduction in albedo. When PV panels are installed on white-roofed buildings, such as those commonly found in regions of Greece or India, the resulting albedo change differs markedly from installations on dark roofs because the albedo of white roofs is a lot higher. Ice and snow have the highest albedo of all surfaces considered, and reflect a large fraction of incoming solar radiation. Consequently, alpine PV installations are associated with the most pronounced albedo changes, resulting in substantially lower reflectivity.

While the albedo reduction introduced by PV installations may increase local heat absorption at the building scale, this effect must be evaluated in conjunction with the benefits of renewable electricity generation. Overall, the literature review (see Section 2.2 in particular) indicates that although replacing natural surfaces with PV panels leads to a measurable albedo effect that can be quantified within an LCA, this effect represents a substantially smaller environmental impact compared to the benefits associated with the renewable energy produced by PV systems. This conclusion is expected to hold true across installations on all surface types including ice and snow where albedo changes are most pronounced. The only existing study about an alpine PV installation in Tibet (see Section 2.3) found that while surface albedo was reduced and net radiation was increased as expected, the PV panels also caused a multitude of other effects such as the soil frozen period to extend significantly and recommended more long-term monitoring and analysis. This data can build the base for a full LCA.

4.1 Data uncertainty and validation

In an LCA, data quality indicators (DQIs) as defined in International Organization for Standardization (2006b) are criteria used to describe, assess, and document how reliable and representative the data feeding into a life cycle inventory can be considered to understand how much confidence can be placed in the LCA results. DQIs cover the following aspects:

1. Technological representativeness: the degree to which the data reflects the actual technology or process studied.
2. Geographical representativeness: how closely the data matches the geographic location of the system (e.g., regional vs. global average conditions).
3. Temporal representativeness: how current the data are relative to the reference year of the study.
4. Completeness: whether all relevant inputs and outputs are included in the data.
5. Reliability and precision: the quality of the given data sources and methods. Measured data is preferred over calculated data. If neither is available, a fallback to estimated or assumed data will be performed.

6. Consistency and methodological coherence: whether the data was generated using consistent assumptions, system boundaries, and methods.

Satellite-derived albedo products generally rank high on all DQI dimensions because they provide granular data that is representative on all the three given dimensions and also complete, reliable, and consistent. Also, they originate from authoritative bodies like NOAA and EUMETSAT and are therefore considered scientifically validated and reliable.

However, satellite-derived albedo products are subject to uncertainties inherently arising from several sources (cf. literature study in Section 2.8):

- The first source of uncertainty originates from technical constraints. If the satellite's pixel size is too coarse for the PV farm to be analysed, mixed pixels that only partly cover the area of interest will influence the results. Inconsistencies can also occur due to a difference between aerial and ground level viewpoints. Finally, sensor calibration is important to avoid introducing long-term drift in data quality in continuous monitoring setups which would affect temporal representativeness.
- Furthermore, operational issues such as temporary sensor malfunctions causing data gaps and/or faulty data are inevitable. This must be explicitly addressed within the suggested methodological framework.
- Another source of uncertainty are atmospheric and environmental variations. Cloud cover is a major challenge for surface albedo estimation, often requiring sophisticated probability-based correction methods. Similarly, snow cover and seasonal vegetation dynamics can drastically alter reflectivity, requiring temporal aggregation to obtain stable, meaningful results. Atmospheric correction is required since variations in aerosols and water vapour can lead to an emerging darkening or brightening in satellite observations, which makes the isolation of the albedo effect from other atmospheric signals complicated.

The simplest approach to cross-validation is to perform it against the generalized data as described in Section 3.4.1.2, or against other available datasets.

4.2 Limitations

The surface albedo numbers compiled in Table 3 have high coverage but do not constitute an exhaustive list. For some use cases, additional literature study might be necessary. Careful analysis is required since the values found in literature are not always of the same type. Sometimes they are yearly means, but they can also be individual data samples. For some surfaces this is not relevant, but for those where seasonal effects play a role it is important. For some use cases and/or land cover types, albedo ground measurements might be required.

The exact approach chosen for the filtering and aggregation steps described in Section 3.4.1.1 has significant impact on the resulting numbers. Therefore, it needs to be carefully designed

and documented, which was omitted in this work but is required for an accurate assessment of the impacts of land cover change in an LCA.

5 Appendix

5.1 Acknowledgements

Many thanks to Daija Angeli and René Itten for extremely valuable feedback and input to earlier versions of this paper, which improved its quality significantly.

5.2 Project organization

Meeting notes can be found in this document (access upon request). The time plan for the project can be found in this document (access upon request)

5.3 Overview: Satellite data for earth observation

This chapter provides an introduction to satellites that provide observational data of the earth for environmental monitoring. The many other existing use cases for satellites in communication, broadcasting, navigation, and for military purposes will not be discussed.

Table 4: Methods for sensing

Method	Key feature	Works at night	Cloud penetrating
Optical (incl. Near-Infrared, NIR)	Reflects sunlight	No	No
Thermal Infrared (IR)	Detects heat	Yes	No
Synthetic Aperture Radar (SAR)	Uses radar	Yes	Yes

There are several different types of methods to sense the data: optical, thermal, and radar based as summarized in Table 4. Optical methods detect sunlight reflected by clouds, land, and oceans, e.g., for red and blue visible light reflectance. Near-infrared (NIR) and infrared (IR) is invisible to the human eye. NIR is strongly reflected by vegetation, and absorbed by water. Therefore, NIR based methods make land cover, plant health, and boundaries between land and water easy to detect. IR detects thermal radiation, i.e. heat, emitted from the earth and atmosphere at day and night. This is useful for observation of temperature and moisture

or dryness as well as atmospheric gaseous water vapor. Synthetic Aperture Radar (SAR) is an active method that works at night and through clouds (unlike the other methods). It detects surface structure and moisture.

At a high level, satellites can be categorized based on their orbital types, which determine their position and altitude, and consequently coverage and purpose:

1. Low Earth Orbit (LEO) satellites orbit at altitudes between 160 and 2.000 kilometers. They are known for their high resolution data. A subset of them, polar orbits, pass over the earth's poles and provide global coverage as the planet rotates beneath them. Another subset is sun-synchronous orbits, which maintain a consistent position relative to the sun, allowing satellites to observe the earth under similar lighting conditions with each pass.
2. Medium Earth Orbit (MEO) satellites operate at altitudes ranging above 2.000 and below 35.000 kilometers. They are typically used for navigation services such as devised based on Assisted Global Navigation Satellite Systems as defined in (3rd Generation Partnership Project (3GPP), 2019), which rely on acquiring and decoding satellite signals to determine their position.
3. Geostationary Earth Orbit (GEO) satellites are located above the equator at 35.786 kilometers, which matches the earth's rotation period, to provide continuous observation of a fixed region of the earth. They are known for providing low resolution data with high update frequency. The data provided is often used for weather and broad climate monitoring.

Each of these orbital satellite types serves different purposes. The satellite orbital types most common for earth observation are LEO and GEO satellites. In the following, an overview of available public domain and commercial observational satellite data of these types that could potentially be relevant for LCA is provided.

5.3.1 Geostationary Earth Orbit (GEO) satellites

Observational Geostationary Earth Orbit satellites provide continuous, real-time monitoring of atmospheric conditions, cloud cover, sea surface temperatures, and solar radiation over large fixed regions. They have lower spatial resolution compared to LEO satellites, but this is being compensated by providing high temporal resolution. Table 5 provides an overview of the existing GEO satellites, their operators, the regions covered, the type of access and, if relevant, the license that the data is available under.

Table 5: GEO satellites overview

Satellite / Series	Operator / Agency	Region Covered	Licensing
GOES series (GOES-16, GOES-17, GOES-18)	NOAA (USA)	Americas	Most data available under NOAA's data policy
Meteosat (MSG and MTG series)	EUMETSAT (Europe)	Europe, Africa, Atlantic Ocean	Open access under EUMETSAT's data policy
Himawari series (8 and 9)	JMA (Japan)	Asia-Pacific region	Open access for research and public use
INSAT/GSAT series (INSAT-3D, INSAT-3DR)	ISRO (India)	Indian subcontinent	Limited public access
Fengyun series (FY-2, FY-4)	CMA (China)	Asia-Pacific region	Restricted access for partners
Electro-L series	Russian Space Agency	Russia, Europe, parts of Asia	Limited public access

The three satellite series where data that is accessible under open licenses offer data delivery frequencies between 5 and 15 minutes for full images. They provide similar imaging capabilities: 16 spectral ranges of wavelengths, called bands or channels, collected by the satellite sensor as discrete portions of the electromagnetic spectrum. Each series provides comparable numbers of optical, near-infrared and infrared channels.

They support rapid scan modes for their regions of focus with data delivery frequencies between 30 seconds and 5 minutes. These are used for detecting fast-changing weather and environmental events such as storms, tornadoes, wildfires and volcanic eruptions, and for short-term weather forecasting (called now-casting).

To summarize, GEO satellites for earth observation are most helpful for high-frequency monitoring of large-scale land and ocean processes.

5.3.2 Low Earth Orbit (LEO) satellites

Far more LEO satellites for earth observation than GEO satellites exist: around 35 GEO satellites compared to around 1000 LEO satellites. Table 6 provides a non-exhaustive listing of the most relevant providers together with the resolution and revisit frequency of the data provided. Note that some providers have more than one satellite on offer. In these cases only the one with the highest resolution and revisit frequency is listed. The newest satellites are Biomass from ESA for forest biomass and carbon content monitoring, and FireSat and OroraTech for wildfire detection. The (*) sign indicates future plans.

Table 6: LEO satellites overview

Satellite / provider	Access	Resolution	Revisit Frequency
Landsat 8 & 9	open	15 – 30 m multispectral	8 days (combined)
Sentinel-1 (A & B/C)	open	5 – 20 m SAR	6 days (combined)
Sentinel-2 (A, B & C)	open	10 – 60 m multispectral	5 days (combined)
MODIS (Terra, Aqua)	open	250 m – 1 km multispectral	Daily
VIIRS	open	375 m – 750 m multispectral	Daily
Biomass	open (*)	10 m P-band SAR	Up to 16 orbits/day
Planet Labs	commercial	3 – 5 m optical	Daily
Maxar WorldView	commercial	30 – 50 cm optical	Up to 15 orbits/day
Airbus	commercial	30 cm optical	1–3 days
Iceye	commercial	0.5 m SAR	Daily to sub-daily
Capella Space	commercial	0.5 m SAR	Daily to sub-daily
GHGSat	commercial	25 m	Variable
FireSat	commercial	5 m thermal IR	30 minutes (*)
OroraTech	commercial	Variable thermal IR	30 minutes (*)

To summarize, LEO satellites play a crucial role in earth observation, particularly for high-resolution and frequent monitoring. The revisit frequency is primarily determined by the size of the satellite constellation. Larger constellations, such as those with over 100 satellites, can achieve revisit frequencies approaching those of geostationary systems.

5.3.3 Data availability for research purposes

While a few public providers offer open-access data with comparatively low resolution, many different commercial options for very high resolution data are on the market. The pricing models of the commercial options depend on the amount of data required and the use case, and are available upon request. Limited opportunities to access the commercial data under a research license exist. The NASA-led Commercial Satellite Data Acquisition Program NASA Earth Science Division (2024) provides access to some of the data for research purposes, most notably for the Maxar WorldView data. It has been used in a number of scientific articles as assessed by Q. Zhao et al. (2022) who conducted a literature study of scientific articles referencing EO satellite missions and found that their number is exponentially growing, and while some cite commercial sources, most of the work is based on the freely available data. In this project, the focus will be on data that is available for research purposes.

References

3rd Generation Partnership Project (3GPP). (2019). *3GPP TS 36.355 V15.3.0 - LTE Positioning Protocol A (LPPa)*. 3GPP.

Argonne National Laboratory. (2012). *Solar energy development programmatic environmental impact statement*. U.S. Department of Energy.

Barron-Gafford, G. A., Minor, R. L., Allen, N. A., Cronin, A. D., Brooks, A. E., and Pavao-Zuckerman, M. A. (2016). The photovoltaic heat island effect: Larger solar power plants increase local temperatures. *Scientific Reports*, *6*(1), 35070.

Bright, R. M., Cherubini, F., and Strømman, A. H. (2012). Climate impacts of bioenergy: Inclusion of carbon cycle and albedo dynamics in life cycle impact assessment. *Environmental Impact Assessment Review*, *37*, 2–11.

Brutsaert, W. (1984). *Hydrology: An introduction*. Cambridge University Press.

Cai, H., Wang, J., Feng, Y., Wang, M., Qin, Z., and Dunn, J. (2016). Consideration of land use change-induced surface albedo effects in life-cycle analysis of biofuels. *Energy & Environmental Science*, *9*(9), 2855–2867.

Cescatti, A., Marcolla, B., Vannan, S. K. S., Pan, J. Y., Román, M. O., Yang, X., Ciais, P., Cook, R. B., Law, B. E., Matteucci, G., et al. (2012). Intercomparison of MODIS albedo retrievals and in situ measurements across the global FLUXNET network. *Remote Sensing of Environment*, *121*, 323–334.

Coimbra, C. F. (2025). Energy meteorology for the evaluation of solar farm thermal impacts on desert habitats. *Advances in Atmospheric Sciences*, *42*(2), 313–326.

Cosgun, A. E., and Demir, H. (2024). Investigating the effect of albedo in simulation-based floating photovoltaic system: 1 MW bifacial floating photovoltaic system design. *Energies*, *17*(4), 959.

Datseris, G., and Stevens, B. (2021). Earth's albedo and its symmetry. *AGU Advances*, *2*(3), e2021AV000440.

David, M., Loog, K., Bortoli, A. de, and Saunier, F. (2025). Nature-based solutions toward net-zero: Surface albedo matters! Demonstration on the case of carbon credits. *Proceedings of the 12th International Conference on Life Cycle Management*.

Diamond, M. S., Gristey, J. J., and Feingold, G. (2024). Testing cloud adjustment hypotheses for the maintenance of earth's hemispheric albedo symmetry with natural experiments. *Geophysical Research Letters*, *51*(20), e2024GL111733.

Dorber, M., May, R., and Verones, F. (2018). Modeling net land occupation of hydropower reservoirs in norway for use in life cycle assessment. *Environmental Science & Technology*, *52*(4), 2375–2384.

ecoinvent Centre. (2023). *Ecoinvent database (version 3.x)*. Swiss Centre for Life Cycle Inventories, St. Gallen, Switzerland.

Forster, P., Storelvmo, T., Armour, K., Collins, W., Dufresne, J.-L., Frame, D., Lunt, D. J., Mauritsen, T., Palmer, M. D., Watanabe, M., Wild, M., and Zhang, H. (2021). The earth's energy budget, climate feedbacks, and climate sensitivity. In V. Masson-Delmotte, P. Zhai, A. Pirani, S. L. Connors, C. Péan, S. Berger, N. Caud, Y. Chen, L. Goldfarb, M. I. Gomis, M.

Huang, K. Leitzell, E. Lonnoy, J. B. R. Matthews, T. K. Maycock, T. Waterfield, O. Yelekçi, R. Yu, and B. Zhou (Eds.), *Climate change 2021: The physical science basis* (pp. 923–1054). Cambridge University Press. https://doi.org/10.1017/9781009157896.009

Fthenakis, V. M., Kim, H. C., and Alsema, E. (2008). Emissions from photovoltaic life cycles. *Environmental Science & Technology*, *42*(6), 2168–2174.

Geyer, R., Lindner, J. P., Stoms, D. M., Davis, F. W., and Wittstock, B. (2010). Coupling GIS and LCA for biodiversity assessments of land use: Part 2: Impact assessment. *The International Journal of Life Cycle Assessment*, *15*(7), 692–703.

Geyer, R., Stoms, D. M., Lindner, J. P., Davis, F. W., and Wittstock, B. (2010). Coupling GIS and LCA for biodiversity assessments of land use: Part 1: Inventory modeling. *The International Journal of Life Cycle Assessment*, *15*(5), 454–467.

Gruber, A., De Lannoy, G., Albergel, C., Al-Yaari, A., Brocca, L., Calvet, J.-C., Colliander, A., Cosh, M., Crow, W., Dorigo, W., et al. (2020). Validation practices for satellite soil moisture retrievals: What are (the) errors? *Remote Sensing of Environment*, *244*, 111806.

Gul, M., Kotak, Y., Muneer, T., and Ivanova, S. (2018). Enhancement of albedo for solar energy gain with particular emphasis on overcast skies. *Energies*, *11*(11), 2881.

Hasler, N., Williams, C. A., Denney, V. C., Ellis, P. W., Shrestha, S., Terasaki Hart, D. E., Wolff, N. H., Yeo, S., Crowther, T. W., Werden, L. K., et al. (2024). Accounting for albedo change to identify climate-positive tree cover restoration. *Nature Communications*, *15*(1), 2275.

Hotelling, H. (1933). Analysis of a complex of statistical variables into principal components. *Journal of Educational Psychology*, *24*(6), 417–441. https://doi.org/10.1037/h0071325

International Organization for Standardization. (2006a). *ISO 14040:2006 Environmental management – Life cycle assessment – Principles and framework*. International Organization for Standardization.

International Organization for Standardization. (2006b). *ISO 14044:2006 Environmental management – Life cycle assessment – Requirements and guidelines*. International Organization for Standardization.

Itten, R., Götz, M., and Kröhnert, H. (2023). Remote sensing based data products for large scale life cycle inventory models. *11th International Conference on Life Cycle Management (LCM), Lille, France, 6-8 September 2023*.

Ji, C., Zhang, Z., Masuda, T., Kudo, Y., and Guo, L. J. (2019). Vivid-colored silicon solar panels with high efficiency and non-iridescent appearance. *Nanoscale Horizons*, *4*(4), 874–880.

Jian, X., Zhang, X., Liu, X., Chen, K., Huang, T., Tao, S., Liu, J., Gao, H., Zhao, Y., Zhugu, R., et al. (2025). Highly resolved satellite-remote-sensing-based land-use-change inventory yields weaker surface-albedo-induced global cooling. *Atmospheric Chemistry and Physics*, *25*(7), 4251–4268.

Jungbluth, N., Stucki, M., Flury, K., Frischknecht, R., and Büsser, S. (2012). Life cycle inventories of photovoltaics. *ESU-Services Ltd.: Uster, Switzerland*, *250*.

Karlsson, C., Miliutenko, S., Björklund, A., Mörtberg, U., Olofsson, B., and Toller, S. (2017). Life cycle assessment in road infrastructure planning using spatial geological data. *The International Journal of Life Cycle Assessment*, *22*. https://doi.org/10.1007/s11367-016-1241-3

Langsdale, M., Verhoelst, T., Povey, A., Schutgens, N., Dowling, T., Lambert, J.-C., Comper-

nolle, S., and Kern, S. (2025). The challenges and limitations of validating satellite-derived datasets using independent measurements: Lessons learned from essential climate variables. *Surveys in Geophysics*, 1–38.

Lavaert, C., Willockx, B., Cappelle, J., and Jung, J. (2023). Influence of the albedo on agrivoltaics electricity production. *AGRIVOLTAICS WORLD CONFERENCE 2023*, *2*.

Li, J., Tian, Y., Zhang, Y., and Xie, K. (2021). Spatializing environmental footprint by integrating geographic information system into life cycle assessment: A review and practice recommendations. *Journal of Cleaner Production*, *323*, 129113.

Li, P., Gao, X., Li, Z., and Zhou, X. (2022). Physical analysis of the environmental impacts of fishery complementary photovoltaic power plant. *Environmental Science and Pollution Research*, *29*(30), 46108–46117.

Li, Z., Zhao, Y., Luo, Y., Yang, L., Li, P., Jin, X., Jiang, J., Liu, R., and Gao, X. (2022). A comparative study on the surface radiation characteristics of photovoltaic power plant in the gobi desert. *Renewable Energy*, *182*, 764–771.

Liang, S. (2001). Narrowband to broadband conversions of land surface albedo i: algorithms. *Remote Sensing of Environment*, *76*(2), 213–238.

Loeb, N. G., Thorsen, T. J., Kato, S., Rose, F. G., Hodnebrog, Ø., and Myhre, G. (2025). Emerging hemispheric asymmetry of earth's radiation. *Proceedings of the National Academy of Sciences*, *122*(40), e2511595122.

Manninen, T., Jääskeläinen, E., Siljamo, N., Riihelä, A., and Karlsson, K.-G. (2022). Cloud-probability-based estimation of black-sky surface albedo from AVHRR data. *Atmospheric Measurement Techniques*, *15*(4), 879–893.

Moretti, L., Cantisani, G., Carpiceci, M., D'Andrea, A., Del Serrone, G., Di Mascio, P., and Loprencipe, G. (2021). Effect of sampietrini pavers on urban heat islands. *International Journal of Environmental Research and Public Health*, *18*(24), 13108.

NASA Earth Science Division. (2024). *Commercial smallsat data acquisition (CSDA) program*. https://www.earthdata.nasa.gov/esds/csdap.

Nemecek, T., Bengoa, X., Lansche, J., Mouron, P., Rossi, V., and Humbert, S. (2014). *World food LCA database methodological guidelines for the life cycle inventory of agricultural products*. https://link.ira.agroscope.ch/en-US/publication/34029

Nemet, G. F. (2009). Net radiative forcing from widespread deployment of photovoltaics. *Environmental Science & Technology*, *43*(6), 2173–2178.

Oke, T. R. (1987). *Boundary layer climates* (2nd ed.). Routledge.

Paris, C., Martinez-Sanchez, L., Velde, M. van der, Sharma, S., Sedona, R., and Cavallaro, G. (2023). Accuracy assessment of land-use-land-cover maps: The semantic gap between in situ and satellite data. *Image and Signal Processing for Remote Sensing XXIX*, *12733*, 187–200.

Reinhard, J., Zah, R., and Hilty, L. M. (2016). Regionalized LCI modeling: A framework for the integration of spatial data in life cycle assessment. In *Advances and new trends in environmental informatics: Stability, continuity, innovation* (pp. 223–235). Springer.

Richardson, K., Steffen, W., Lucht, W., Bendtsen, J., Cornell, S. E., Donges, J. F., Drüke, M., Fetzer, I., Bala, G., Von Bloh, W., et al. (2023). Earth beyond six of nine planetary boundaries. *Science Advances*, *9*(37), eadh2458.

Riihelä, A., Jääskeläinen, E., and Kallio-Myers, V. (2024). Four decades of global surface albedo estimates in the third edition of the CM SAF cLoud, albedo and surface radiation (CLARA) climate data record. *Earth System Science Data*, *16*(2), 1007–1028.

Roccetti, G., Bugliaro, L., Gödde, F., Emde, C., Hamann, U., Manev, M., Sterzik, M. F., and Wehrum, C. (2024). HAMSTER: Hyperspectral albedo maps dataset with high spatial and TEmporal resolution. *Atmospheric Measurement Techniques*, *17*(20), 6025–6046.

Schaaf, C., and Wang, Z. (2021). *MODIS/terra+aqua BRDF/albedo black sky albedo shortwave daily L3 global 30ArcSec CMG V061* [Dataset]. NASA Land Processes Distributed Active Archive Center (LP DAAC). https://doi.org/10.5067/MODIS/MCD43D51.061

Survey, U. S. G. (2020). *Landsat surface reflectance product* [Dataset]. U.S. Geological Survey. https://www.usgs.gov/landsat-missions/landsat-surface-reflectance

Susca, T. (2012). Enhancement of life cycle assessment (LCA) methodology to include the effect of surface albedo on climate change: Comparing black and white roofs. *Environmental Pollution*, *163*, 48–54.

Tetzlaff, G. (1983). Albedo of the sahara. In *Cologne university satellite measurement of radiation budget parameters* (pp. 60–63). University of Cologne.

Tran, B. N., Van Der Kwast, J., Seyoum, S., Uijlenhoet, R., Jewitt, G., and Mul, M. (2023). Uncertainty assessment of satellite remote-sensing-based evapotranspiration estimates: A systematic review of methods and gaps. *Hydrology and Earth System Sciences*, *27*(24), 4505–4528.

U.S. Environmental Protection Agency. (2003). *Heat island reduction initiative: Cool roofs*. U.S. EPA. https://www.epa.gov/sites/default/files/2014-06/documents/hiribrochure.pdf

Van Dalum, C. T., Van De Berg, W. J., Lhermitte, S., and Van Den Broeke, M. R. (2020). Evaluation of a new snow albedo scheme for the greenland ice sheet in the regional atmospheric climate model (RACMO2). *The Cryosphere*, *14*(11), 3645–3662.

Wang, S., Meng, X., Li, Q., Li, Z., Yang, P., Niu, W., and Shang, L. (2025). Environmental impacts of pastoral-integrated photovoltaic power plant in an alpine meadow on the eastern tibetan plateau. *Atmospheric Chemistry and Physics*, *25*(18), 11301–11315.

Wei, S., Ziegler, A. D., Qin, Y., Wang, D., Chen, Y., Yan, J., and Zeng, Z. (2024). Small reduction in land surface albedo due to solar panel expansion worldwide. *Communications Earth & Environment*, *5*(1), 474.

Wu, S., Lin, X., Bian, Z., Lipson, M., Lafortezza, R., Liu, Q., Grimmond, S., Velasco, E., Christen, A., Masson, V., et al. (2024). Satellite observations reveal a decreasing albedo trend of global cities over the past 35 years. *Remote Sensing of Environment*, *303*, 114003.

Xu, Z., Li, Y., Qin, Y., and Bach, E. (2024). A global assessment of the effects of solar farms on albedo, vegetation, and land surface temperature using remote sensing. *Solar Energy*, *268*, 112198.

Zanaga, Daniele., Van De Kerchove, Ruben., Daems, Dirk., De Keersmaecker, Wanda., Brockmann, Carsten., Kirches, Grit., Wevers, Jan., Cartus, Oliver., Santoro, Maurizio., Fritz, Steffen., Lesiv, Myroslava., Herold, Martin., Tsendbazar, N.-E., Xu, Panpan., Ramoino, Fabrizio., and Arino, Olivier. (2022). *ESA WorldCover 10 m 2021 v200* (Version v200) [Dataset]. Zenodo. https://doi.org/10.5281/zenodo.7254221

Zhang, X., and Xu, M. (2020). Assessing the effects of photovoltaic powerplants on surface temperature using remote sensing techniques. *Remote Sensing*, *12*(11), 1825.

Zhao, Q., Yu, L., Du, Z., Peng, D., Hao, P., Zhang, Y., and Gong, P. (2022). An overview of the applications of earth observation satellite data: Impacts and future trends. *Remote Sensing*, *14*(8), 1863.

Zhao, S., Zhang, X., and Jin, X. (2025). Comparative evaluation of cool roofs and photovoltaic roofs in sustainable buildings within the scope of the 3-e static payback period framework. *Buildings*, *15*(19), 3500.

Zhou, Y., Marathe, S., Zeman, M., Isabella, O., and Ziar, H. (2025). Assessing the dual radiative consequences of urban PV integration: Albedo change and radiative forcing dynamics. *Applied Energy*, *401*, 126544.

Zhu, Q., Chen, J., Wu, L., Huang, Y., Shao, C., Dong, G., Xu, Z., and Li, X. (2024). Changes in albedo and its radiative forcing of grasslands in east asia drylands. *Ecological Processes*, *13*(1), 1–15.